

## Thermal Shock as an Ice Multiplication Mechanism. Part II. Experimental

W. D. KING<sup>1</sup> AND N. H. FLETCHER

*Department of Physics, University of New England, Armidale, NSW, Australia*

(Manuscript received 19 May 1975, in revised form 18 September 1975)

### ABSTRACT

Thermal shock tests were conducted on large numbers of ice spheres and plates, all of macroscopic size. The thermal shock was applied by cooling the specimens to the desired temperature, and then rapidly warming part of one surface by bringing water in contact with it. The spheres had a median cracking temperature of  $-16^{\circ}\text{C}$ , and comparison with thermoelastic theory yielded tensile strength values for ice in the range 20–30 bars. Initiation of cracking in thick plates was a function of the temperature and of the ratio  $a/b$  (ratio of radius of warmed area to that of the cylindrical plate). For  $a/b=0.6$ ,  $-20^{\circ}\text{C}$  was the critical temperature, but for  $a/b<0.2$ , which is a more appropriate scaling factor in terms of riming of cloud particles, the samples had to be colder than  $-35^{\circ}\text{C}$  before any cracks appeared. None of the samples fragmented or separated. Because the experimentally applied temperature changes were more severe than would be experienced by rimed ice crystals in clouds, it is concluded that thermal shock is unlikely to be an important ice multiplication mechanism at  $-5^{\circ}\text{C}$ .

### 1. Introduction

In Part I of this study (King and Fletcher, 1976) quasi-static thermoelastic theory was used to calculate stresses in ice crystals when part of one surface was warmed to  $0^{\circ}\text{C}$ , in simulation of riming of the crystal by a cloud droplet. This theory was used in conjunction with the Griffith conditions for brittle fracture to calculate the temperature at which the ice crystal could be expected to fracture. Within this theoretical framework, the important scaling factor in determining the susceptibility of the crystal to failure by this mechanism was found to be the ratio of crystal to droplet sizes, the thermal stresses being a maximum for large drops and thin plates. For the usual riming situation, where the crystal is much larger than the riming droplet, it was calculated that the crystal would have to be initially colder than  $-35^{\circ}\text{C}$  before fracture could be expected. Large drop, thin plate combinations were the most sensitive, requiring about  $-10$  to  $-15^{\circ}\text{C}$  to induce cracking, while columns, needles and thick plates belonged to an intermediate class whose critical temperature was about  $-20^{\circ}\text{C}$ .

In this paper, we present the results of thermal shock experiments on large ice samples, and compare the findings with the predictions of Part I.

In quite general terms, investigations of the mechanical properties of brittle materials are hampered by the variability of results inherently associated with the

nature of brittle failure. The statistical aspect of this failure is well recognized, and indeed, the Griffith theory assumes the presence of randomly distributed flaws. In part, the variability in results can be overcome by performing large numbers of experiments, an approach which, in the present context, dictated the use of large-grained multi-crystalline samples. Although single crystals are the most appropriate to use in terms of simulating cloud particles, they are time consuming to grow and it is questionable whether their brittle failure would be any more consistent than with polycrystalline samples anyway. Large-grained polycrystals (typical grain size about  $1\text{ cm}^3$ ) represent a compromise in that they can be prepared with comparative ease and grain boundary effects are minimal. Some previous experiments on thermal shock in ice (Gold, 1963) established that crack nucleation was independent of grain size provided the grains were larger than  $(0.15\text{ cm})^3$ .

### 2. Conditions on the water temperature

In clouds, the collision between a supercooled water drop and an ice crystal results in the impact area being warmed to  $0^{\circ}\text{C}$  and the rapid freezing of a small portion of the drop. Because of the difficulties associated with the production and handling of supercooled water in the laboratory, water warmer than  $0^{\circ}\text{C}$  was used to produce the thermal shock in our experiments. While the interfacial temperature under these conditions is still  $0^{\circ}\text{C}$ , it is not immediately clear whether this is achieved by melting a little of the surface layer of ice, the very region where the stresses are usually quite

<sup>1</sup> Present affiliation: Division of Cloud Physics, CSIRO, Sydney, Australia.

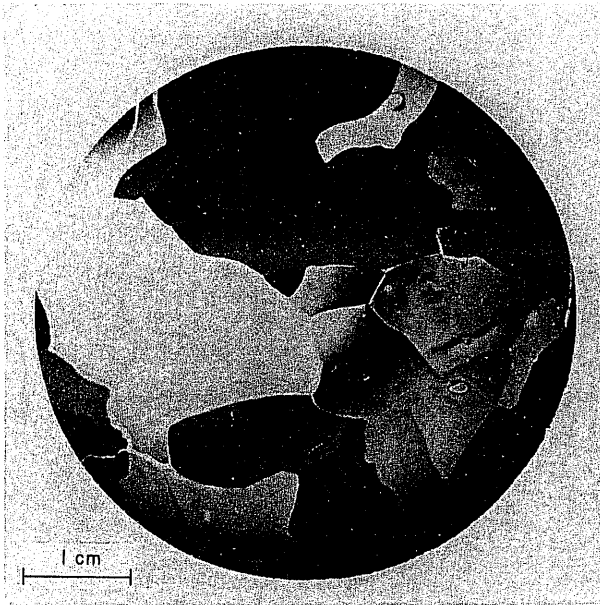


FIG. 1. Thin section of a 5.0 cm slab under polarized light.

high, or by freezing some of the water in contact with the ice. Although the final equilibrium state of the thermally isolated system depends on the relative mass of the two phases present, the question of whether the ice substrate grows or melts is primarily fixed by the initial temperatures of the ice and water. A full discussion of this problem involves the concepts of a moving or free boundary and is outside the scope of this study, but it is proposed that the required information be obtained as follows. When a sphere of thermal conductivity  $k_1$ , thermal diffusivity  $\kappa_1$ , and at a uniform temperature  $T_1$  is immersed in a large volume of liquid described by similar quantities  $k_2$ ,  $\kappa_2$  and  $T_2$ , then it can be shown that in the limit as  $t \rightarrow 0$ , the surface temperature of the sphere takes the value of  $T_s$ , where

$$T_s = T_1 + \frac{(T_2 - T_1)}{(1 + k_1 \sqrt{\kappa_2} / k_2 \sqrt{\kappa_1})}. \quad (1)$$

A similar result holds for semi-infinite geometry (Carslaw and Jaeger, 1959, p. 88) and, using fairly crude arguments, one can show that it also applies to any situation where the heat flow is normal to the interfacial surface. Eq. (1) is valid for cases in which there is no phase change between  $T_1$  and  $T_2$ , and for the ice-water system we have interpreted it as follows. If the predicted surface temperature  $T_s$  is greater than  $0^\circ\text{C}$ , some of the ice surface will melt, and conversely, if the predicted temperature  $T_s$  is less than  $0^\circ\text{C}$ , then water in contact with the ice will freeze. If we wish to simulate the riming situation in which the liquid always freezes, then (1) places restrictions on the temperature of the water that can be placed on the ice. With appropriate values for the thermal properties of ice and water,

this condition is described by

$$T_2 < -1.27T_1, \quad (2)$$

where  $T_1$  and  $T_2$  are both measured in degrees Celsius.

It is an interesting by-product that these concepts can be used to qualitatively explain the "stickiness" of ice at cold temperatures. At temperatures warmer than about  $-15^\circ\text{C}$ , ice feels slippery when touched, whereas at temperatures colder than this, it tends to be sticky and adheres to the fingers. If this stickiness is interpreted as being due to the instantaneous freezing of surface moisture on the skin, and we take the temperature of the moisture to be close to room temperature, then (1) predicts that ice will be sticky at temperatures lower than  $-16^\circ\text{C}$ , in reasonable agreement with practical experience.

### 3. Experimental method

#### a. Sample preparation

Air-free columnar ice was prepared by allowing water to freeze slowly in an insulated container in a cold room at  $-10^\circ\text{C}$ . Growth rates were about  $1 \text{ mm h}^{-1}$ . The water was once-distilled and contained ionic impurities to the extent that the resistivity was  $10^8 \Omega \text{ m}$ . Fig. 1, showing a thin section of the ice between polaroids, gives an indication of grain size. Circular slabs and thin disks of uniform diameter were obtained from ice grown in this manner by cutting with a stainless steel hole saw to the required depth, and then removing the excess by melting. The slabs were 5.0 cm in diameter and 1.7 cm thick, and the thin disks 5.0 cm in diameter and 1–2 mm thick.

To achieve a well-defined warmed area on the surface of the slab or disk, a thin-walled perspex (lucite) annulus of the desired size was placed on the ice and a thin film of water used to freeze it into position. Young's modulus for perspex is approximately half that of ice, and the thin walls (typically 1.5 mm) ensured that any perturbations to the stress system were negligible. The perspex rings were 3 mm high, and the water contained in them took about 5 min to freeze—ample time to establish the temperature distributions.

Spheres 2.0 and 3.0 cm in diameter were grown in plastic molds which were available commercially for making cocktail ice. Variations in diameter due to mold imperfections were of the order of 5%. Air-free specimens were obtained by intermittently vacuum-degassing the water for about 6 h, and then freezing this water in the molds inside a sealed aluminum vacuum chamber. Spheres obtained by freezing the water while exposed to air contained air bubbles at a concentration of approximately  $20 \text{ cm}^{-3}$ . Both clear and bubbly spheres were used in the experiments to try to gauge the effects of the air bubbles on the cracking activity.

*b. Effect of varying the water temperature*

A series of exploratory experiments, designed to examine whether the water temperature was a variable that influenced the thermal shock, were conducted in the cell shown in Fig 2. This consisted of a long sealed brass tube immersed in a dewar of water-ethylene glycol mixture. The temperature inside the tube was controlled by means of heaters wrapped externally around it. To aid in the detection and timing of cracks, a ceramic microphone insert, the output of which was fed to a tape recorder, was mounted in perspex at the base of the tube and the ice slab rested above this on a 0.05 mm thick copper diaphragm. The required volume of water could be dropped onto the slab by means of a miniature burette and the temperature of the water monitored by a thermocouple mounted inside the burette tip. Temperature corrections to allow for cooling during the free fall from burette to slab were negligible. The temperature of the slab was measured by a thermocouple attached to the copper diaphragm. The temperature difference between the upper and lower surfaces of the ice sample was less than 0.5°C.

The results for this series of experiments, conducted on the thick cylindrical slabs for which  $a/b=0.6$  (where  $a$  and  $b$  are the radii of warmed region and slab respectively) are shown in Fig. 3, where the dashed line refers to the condition expressed by Eq. (2). It is apparent from this figure, provided condition (2) is met, that the water temperature has no influence in determining the thermal shock and associated stresses. As a result of this finding, subsequent experiments were conducted in a simpler fashion, where there was less control over the water temperature, enabling samples to be processed

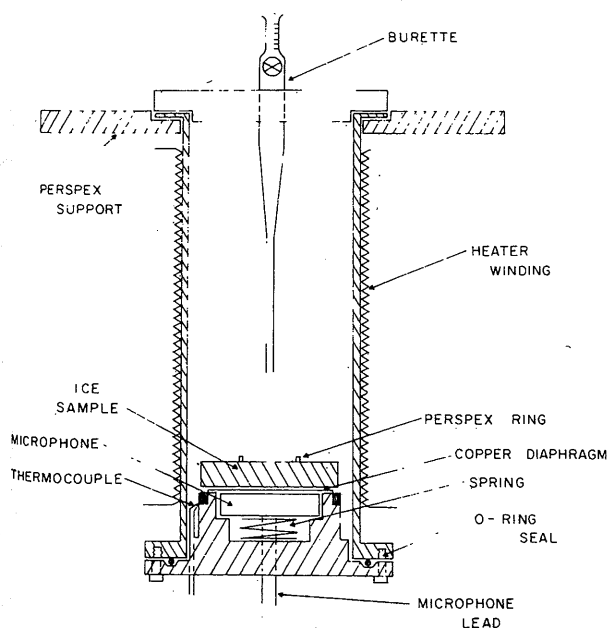


FIG. 2. Schematic diagram of cell used for thermal shock experiments on single slabs.

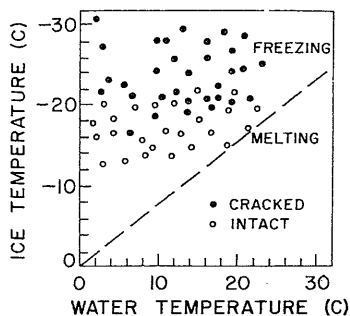


FIG. 3. Thermal shock results for single slabs for which  $a/b=0.6$ . The broken line separates the regions corresponding to initial melting or freezing of the ice surface layer.

more rapidly. Batches of the ice samples, usually 20 or more, were cooled to the desired temperature in a small desk-top refrigerator. Water cooled to a temperature which satisfied (2) was then placed inside the lucite annulus with a syringe. The time to the first crack was noted with a stop watch, a method estimated to be accurate to 0.3 s. The treatment for the spheres was similar, except that they were handled with isothermal tongs and immersed completely in the water. In all, 1000 spheres, 800 slabs and 800 thin disks were tested.

*c. Thermal shock results*

1) SPHERES

The results of the experiments on spheres are shown in Fig. 4, where the fraction of spheres which cracked is shown as a function of their initial temperature. Each point represents the result for a sample of at least 20 spheres. It can be seen that there were no significant variations in cracking activity due to either size or air bubble content. In relation to a size effect, it was shown in Section 8c of Part I that the sphere diameter only plays an important role in determining the time at which the maximum stress is attained, and not the actual value of this stress. The insensitivity to size as shown in Fig. 4 is thus in accordance with the theoretical predictions. We have no explanation, however, of why the presence of air bubbles, which are normally considered stress concentration centers, had no effect on the cracking activity. The consistency of

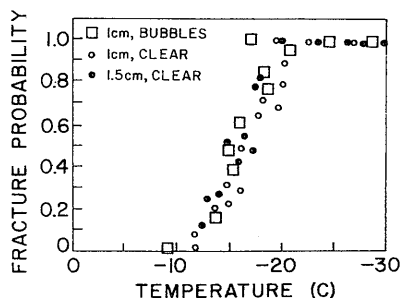


FIG. 4. Variation of fracture probability with temperature for spheres.

the results shown in Fig. 4 suggests that the fracture-determining parameters were inherent properties of the ice structure itself (as opposed to growth defects, etc.) and partly justifies the approach taken.

Fig. 4 shows that the transition to cracking activity was a fairly sharp one: cooling the spheres from  $-14$  to  $-18^\circ\text{C}$  increased the probability of fracture from 0.2 to 0.8 and, for temperatures colder than  $-20^\circ\text{C}$ , substantially all of the spheres cracked. The first crack usually formed below the surface in the region between  $r/b=0.5-0.8$ . These cracks were spherical in shape, concentric with the outer surface, but not closed spheres. For temperatures warmer than  $-20^\circ\text{C}$ , these were normally the only cracks, but at colder temperatures the spherical cracks were often followed by "star" cracks characterized by separation surfaces which were diametral planes of the sphere. The topological nature of these cracks would suggest that they be associated with radial and azimuthal tensile stresses, respectively, and these associations are strengthened by quantitative considerations to be discussed later.

All of the spheres remained intact after cracking; they were remarkably robust and could be dropped from a height of 30 cm onto a desk top without fragmenting. While it was not expected that the incomplete spherical cracks would cause separation, it was a little surprising that some of the slabs divided by five or six star cracks remained intact. It seems likely that after a crack formed, water on the exterior froze and resealed them. It is unlikely that water filled the cracks entirely because white-light interference fringes could be seen in the vicinity of the cracks, indicating that the separation was of the order of  $0.5\ \mu\text{m}$ . This represents a gap of thousands of atomic distances, and implies that macroscopic separation was effected and maintained.

For the large spheres, the time delay between immersion in water and the occurrence of the first crack was measured by listening for the crack and again timing with a stop watch. No results were taken for the smaller spheres because their shorter thermal time constant invariably meant that the first cracks occurred so rapidly that accurate measurements could not be obtained using this method. In general, the time delay decreased with decreasing temperature, and this variation is shown for the large spheres in Fig. 5. The error

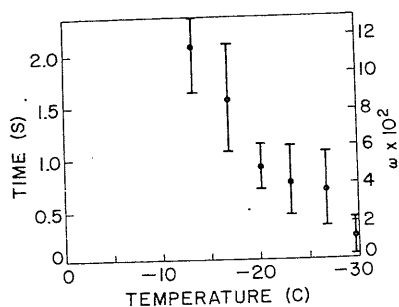


FIG. 5. Time delay to first cracks in 3.0 cm diameter spheres.

bars shown there denote maximum deviations from the average value. Despite the large amount of scatter in the data, it can provide some useful information on cracking stresses when taken in conjunction with the time-dependent stresses calculated for this situation in Section 8c of Part I. If we take the representative critical temperature as the one corresponding to a probability of 0.5 of fracture, then for spheres, this temperature is  $-16^\circ\text{C}$ , at which cracks occur after a delay of  $\omega=10^{-2}$ . Reference to Fig. 7 of Part I shows that the calculated radial stress near this time and for this temperature lies in the range 20 to 30 bars for  $0.5 < r/b < 0.8$ . Although a little higher than the value assumed in Part I, these are reasonable values for the tensile strength of ice and lend weight to the hypothesis that the tensile radial stresses cause the first cracks. At temperatures warmer than  $-20^\circ\text{C}$ , the stress relief afforded by these spherical cracks is probably sufficient to prevent further cracking, but at colder temperatures, the azimuthal stresses are probably responsible for the star cracks. At no temperature was there any evidence to suggest that the initial azimuthal stresses, which were compressive and calculated to be in excess of 100 bars, induced cracking.

A casual inspection of the calculations of Section 8c of Part I would suggest that the theory and experiment disagree on the minimum supercooling required to cause fracture. The calculated maximum radial stress was 2.6 bars, occurring when  $\omega \approx 6 \times 10^{-2}$ . This implies that cracking ought to be induced by temperature changes as small as  $8^\circ\text{C}$  at times up to 10 s after immersion, in contradiction to the results of Figs. 4 and 5. It should be pointed out, however, that the volume of the sphere which experiences a given magnitude of the tensile stress decreases with the temperature difference until, at the temperature of  $-8^\circ\text{C}$  mentioned above, the critical stress of 20 bars is attained at only one point—the center of the sphere. It appears that the strain energy associated with a reduced volume is insufficient to nucleate cracks at temperatures warmer than  $-16^\circ\text{C}$ .

To sum up, spheres require  $16 \pm 4$  degrees of supercooling before failure occurs, and the critical stress is in the range 20–30 bars. It is an interesting, but quite irrelevant, consequence of this, that if ice of general spherical shape feels sticky to the touch, then it will probably crack when placed in water.

## 2) THICK SLABS

The results for slabs with three different sized warmed areas are shown in Fig. 6. It shows a fairly strong size dependence, the 0.5 probability points being  $-24$  and  $-19^\circ\text{C}$  for  $a/b=0.4$  and  $0.6$ , respectively; for  $a/b=0.2$ , it is lower than  $-40^\circ\text{C}$ , the coldest temperature at which results could conveniently be taken.

The cracks were normal to the warmed slab surface, i.e., parallel to the predominant  $c$ -axis direction. Although they penetrated the slab completely, the slabs

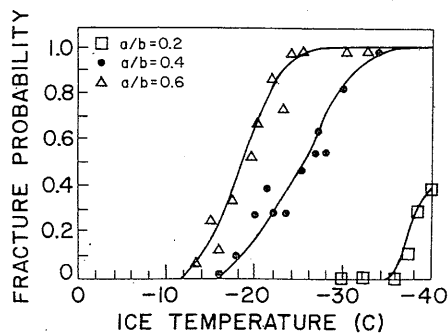


FIG. 6. Fracture probability for thick slabs.

always remained intact and were again difficult to separate into the separate cracked regions. Fig. 7 shows a photograph of the crack system in a slab cracked at  $-25^{\circ}\text{C}$ . Although the cracking behavior was not studied in any detail, it was obvious that several of the features described by Gold (1963), for example the curving of cracks within a single crystal domain and the branching of cracks at grain boundaries, were present.

The time to first cracks was again temperature-dependent and indicated that the instantaneous compressive stresses were not important compared with the delayed bending ones. In terms of  $\omega = \kappa t / b^2$ , a typical delay at  $-20^{\circ}\text{C}$  was  $7 \times 10^{-8}$ . Comparison with the thick plate theory shows that this is reasonable and yields a tensile strength value of about 28 bars. The strong size dependence apparent from Fig. 7 can partly be explained by noting that the geometry of the  $a/b = 0.2$  situation can be described by the semi-infinite model, for which it was estimated that a temperature change in excess of  $35^{\circ}\text{C}$  would be required. The differences between the  $a/b = 0.4$  and  $0.6$  cases, both of which fit into the thick plate category, are probably due to small changes in the  $\tau_{\theta\theta}$  stress with size superimposed on the more constant  $\tau_{rr}$  stresses. This hypothesis is supported by the results of a series of experiments in which the entire surface of the slab was warmed, i.e.,  $a/b = 1$ . In this situation, the  $\tau_{\theta\theta}$  stresses are minimized and the minimum temperature difference shifted to  $24^{\circ}\text{C}$ . In effect, warming more than  $a/b = 0.6$  decreases the  $\tau_{\theta\theta}$  stresses and pushes the critical temperature below  $-20^{\circ}\text{C}$ .

To sum up the results for slabs, it appears that when  $a/b < 0.2$ , the semi-infinite approximation is good and it takes about 40 degrees of supercooling to cause fracture. As the warmed area increases in size, bending and tensile surface stresses increase in importance. The bending stresses attain their maximum value somewhere near  $a/b \approx 0.5$ , and the surface ones around  $a/b \approx 0.7$ . This latter case corresponds to the highest probability of fracture, and requires about 20 degrees of supercooling.

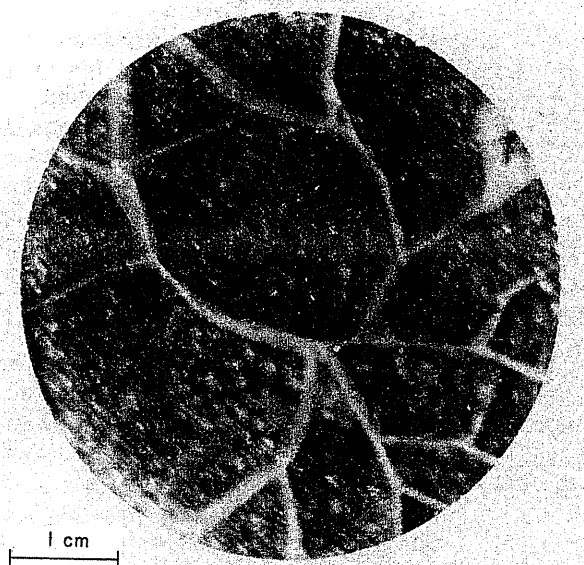


FIG. 7. Typical cracking pattern of a slab.

### 3) THIN PLATES

These results are shown in Fig. 8, the half-probability temperatures being  $-22$ ,  $-13$  and  $-9^{\circ}\text{C}$  for  $a/b$  ratios of 0.2, 0.4 and 0.6, respectively. The scatter in the results can probably be attributed to variations in the thickness of the sample, which varied from 1–2 mm. In general, there was only one crack, occurring after a delay of less than 0.5 s which propagated from the outside edge of the disk toward the center along a radial line, never penetrating far inside the warmed area. These features, along with the pronounced size dependence, correspond qualitatively, at least, to the predictions of the theory of Part I. Quantitative comparisons were difficult to make because the theory was set up for purely radial heat flow, and it is difficult to know when this condition is met experimentally. Despite these difficulties, the calculations are consistent with a tensile strength somewhere in the range 22 to 30 bars.

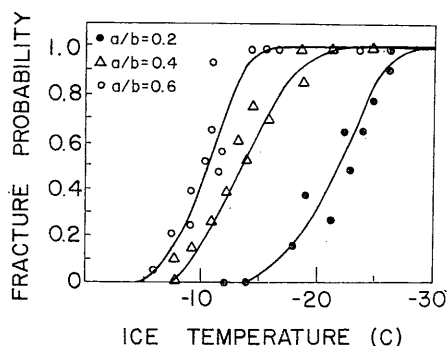


FIG. 8. Fracture probabilities for thin disks.

#### 4. Discussion and conclusions

The results of the experiments on macroscopic crystals essentially confirm the predictions of the quasi-static thermoelastic theory—that the probability of fracture is enhanced as the ratio of warmed area to droplet thickness is increased. Quantitatively, the results for spheres, slabs and thin plates are consistent with a value for the tensile strength of ice which lies somewhere in the range 20–30 bars. Although the upper limit of this range is higher than what is usually obtained from mechanical tests, it is consistent with values found by Gold (1963) during the course of some thermal shock experiments. It may well be that application of a thermal rather than mechanical stress could be a convenient test procedure for measuring the brittle tensile strength of ice, since it does not suffer from the traditional testing problems associated with gripping and aligning the sample.

Given that the thermoelastic theory is found to provide an adequate description of macroscopic processes, one is then faced with the problem of extrapolating to processes on the microscopic scale appropriate to clouds. In Part I, we advanced several reasons why thermal shock should be less severe for particles of the size found in clouds. Briefly, these were: (i) an even higher value for the effective tensile strength of microscopic particles, (ii) the temperature changes in the ice particle due to riming by a droplet  $\lesssim 100 \mu\text{m}$  radius are less severe than those imposed in the theory and experiment, and (iii) having a stress value which exceeds the tensile strength is not a sufficient condition for the generation and propagation of cracks. The experiments outlined above suggest two further reasons why ice multiplication via the thermal shock mechanism is unlikely. First, fracture and crack occurrence do not necessarily imply fragmentation: in all of the experiments, the samples remained intact. While this does not preclude the possibility that micro-splinters were ejected, mechanical fracture would appear to be a prerequisite for splinter ejection, and it has been shown that fracture of crystals at warm temperatures is un-

likely. Second, a direct extrapolation of the most sensitive macroscopic situation, that of a thin plate cracking at  $-10^\circ\text{C}$ , without considering any of the scale-change effects outlined above, would require the collision between a plate  $400 \mu\text{m}$  in diameter with a cloud droplet about  $200 \mu\text{m}$  in diameter. Such an event would be extremely rare.

To sum up, the warmest temperature at which fracture could be experimentally induced by thermal shock was about  $-9^\circ\text{C}$ , and theoretical extrapolations suggest that in clouds this figure should be more like  $-20^\circ\text{C}$ . This particular situation would be very rare, anyway, and the more typical riming situation involving small droplets and large crystals would need to occur below  $-40^\circ\text{C}$  before fracture could be expected. Although no experiments were performed on needles and columns which are known to be the dominant growth habit at the critical ice multiplication of  $-5^\circ\text{C}$ , theoretical considerations given in Section 8b of Part I show that these should behave similarly to plates under thermal shock. It thus seems that some other mechanism must be responsible for the proliferation of ice crystals near  $-5^\circ\text{C}$ .

*Acknowledgments.* This study forms part of a project supported by the Australian Research Grants Committee. One of us (W. D. K.) is also grateful to the Commonwealth Scientific and Industrial Research Organization for a Postgraduate Studentship, during the tenure of which the work, which forms part of a Ph.D. thesis, was performed. The authors are also grateful to the drafting and typing staff of the Department of Atmospheric Science at the University of Wyoming for their assistance.

#### REFERENCES

- Carslaw, H. A., and J. C. Jaeger, 1959: *Conduction of Heat in Solids*. Clarendon Press, Oxford, 510 pp.  
 Gold, L. W., 1963: Cracking of ice plates. *Can. J. Phys.*, **41**, 1712–1728.  
 King, W. D., and N. H. Fletcher, 1976: Thermal shock as an ice multiplication mechanism. Part I. Theory. *J. Atmos. Sci.*, **33**, 85–96.